Dalton Transactions

ROYAL SOCIETY OF CHEMISTRY

PAPER

View Article Online
View Journal | View Issue

Open Access Article. Published on 30 June 2023. Downloaded on 6/13/2026 6:36:53 AM.
This article is licensed under a Creative Commons Attribution-NonCommercial 3.0 Unported Licence.

Check for updates

Cite this: *Dalton Trans.*, 2023, **52**, 10507

Antibacterial properties of phosphine gold(I) complexes with 5-fluorouracil†

Ricardo Ferrando,[a,b] Scott G. Mitchell,[b,c] Elena Atrián-Blasco *[b] and Elena Cerrada *[a]

Received 17th April 2023,
Accepted 30th June 2023

DOI: 10.1039/d3dt01159c

rsc.li/dalton

New gold(I) complexes with coordination to 5-fluorouracil (5-FU), an anticancer drug with antibacterial properties, have been synthesised and characterised, and are the first reported examples of 5-FU–Au compounds. These new complexes show high solution stability, even in the presence of a cysteine derivative, and so were evaluated as antibacterial compounds against model Gram-positive and Gram-negative bacteria. All the complexes show excellent antibacterial activity against Gram-positive *B. subtilis*, most of them improving the activity of 5-FU alone. Furthermore, these new complexes are also active against Gram-negative *E. coli*, where [Au(5-FU)(PTA)], the complex with the smallest phosphane, is the most bactericidal, 32 times more active than 5-FU on its own.

Introduction

5-Fluorouracil (2,4-dihydroxy-5-fluoropyrimidine; 5-FU) is an analogue of the nucleobase uracil with a fluorine atom at the C-5 position. It is used for the treatment of a wide range of cancers: colorectal, breast and head and neck cancers, since the discovery of its activity in 1957.[1] But, it is against colorectal cancer where 5-FU shows the best activity.[2,3] In fact, 5-FU is administered together with leucovorin as co-adjuvants in the treatment of colon cancer with oxaliplatin.[4,5] Its mechanism of action consists of the inhibition of thymidylate synthase, a key enzyme for the production of DNA, in an irreversible manner; and incorporation of its metabolites into RNA and DNA, causing DNA damage.[6] 5-FU is also applied to the treatment of some skin cancers, Bowen's disease and actinic keratosis.[7] In addition to its anticancer properties, 5-FU has been shown to have potent antimicrobial effects against different bacterial pathogens.[8,9] It seems that the effect of 5-FU would be dual by blocking the production of virulence factors and biofilm besides bacterial growth.[10–12]

The discovery of the antimicrobial properties of $K[Au(CN)_2]$ against *Mycobacterium tuberculosis* by R. Koch at the end of the 19th century[13] encouraged researchers to consider gold complexes as potential antibacterial agents. Since then, many examples of gold(I) complexes have shown promising activity against a broad spectrum of microorganisms.[14–17] One of the most studied gold(I) complexes is auranofin (2,3,4,6-tetra-acetyl-1-thio-β-D-glucopyranosato-*S*-triethylphosphane gold(I)), which has been widely studied displaying high efficacy mainly against Gram-positive bacteria, including multidrug-resistant strains.[18–28] As in the case of its anticancer activity, the mechanism of action behind its antibacterial activity is the inhibition of thioredoxin reductase (TrxR).[29]

Although many examples of complexes based on metals such as platinum[30–32] and silver[33–37] coordinated to 5-FU and its derivatives have been studied, to the best of our knowledge, only two examples of gold(I) complexes have been described with 5-FU derivatives (5FdUrd, 5-fluoro-2′-deoxyuridine and Tegafur, 5-fluoro-1-(2-tetrahydrofuryl)-2,4(1*H*,3*H*-pyrimidinedione).[38]

With this background, we describe here the synthesis of new gold(I) 5-fluorouracil complexes, the first reported 5-FU–Au coordination compounds, with the phosphanes PTA (1,3,5-triaza-7-phosphaadamantane), DAPTA (3,7-diacetyl-1,3,7-triaza-5-phosphabicyclo[3.3.1]nonane), PPh_3 (triphenylphosphane) and TPPTS (trisodium 3,3′,3″-phosphanetriyltri(benzene-1-sulfonate). The antibacterial activity of these complexes has been studied against two model bacterial strains, *E. coli* and *B. subtilis*.

Experimental

General

Solvents were used as received without purification or drying. The starting materials $[AuCl(PR_3)]$,[39–41] PTA,[42] DAPTA[43] and

[a]*Departamento de Química Inorgánica, Instituto de Síntesis Química y Catálisis Homogénea-ISQCH, Universidad de Zaragoza-CSIC, 50009 Zaragoza, Spain. E-mail: ecerrada@unizar.es*
[b]*Instituto de Nanociencia y Materiales de Aragón (INMA), CSIC-Universidad de Zaragoza, Zaragoza 50009, Spain. E-mail: e.atrian.blasco@csic.es*
[c]*CIBER de Bioingeniería, Biomateriales y Nanomedicina, Instituto de Salud Carlos III, 28029 Madrid, Spain*

†Electronic supplementary information (ESI) available. See DOI: https://doi.org/10.1039/d3dt01159c

Open Access Article. Published on 30 June 2023. Downloaded on 6/13/2026 6:36:53 AM. This article is licensed under a Creative Commons Attribution-NonCommercial 3.0 Unported Licence.

TPPTS[44] were prepared as previously reported. All other reagents were commercially available and used without further purification. ^{1}H, ^{13}C{^{1}H}, ^{19}F, and ^{31}P{^{1}H} spectra were recorded on a Bruker Avance 400 or a Bruker ARX 300 spectrometer. Chemical shifts (δ, ppm) were reported relative to the solvent peaks in the ^{1}H, ^{13}C spectra or external 85% H_3PO_4 or $CFCl_3$ in ^{31}P or ^{19}F spectra. IR spectra were recorded in the range of 4000–200 cm^{-1} on a PerkinElmer Spectrum 100 spectrophotometer on solid samples using an ATR accessory. C, H, and N analyses were carried out with a PerkinElmer 2400 Series 2 microanalyzer.

Synthesis of the complexes

[Au(5-FU)(PR$_3$)] (PR$_3$ = PTA, 1, DAPTA, 2, PPh$_3$, 3, and TPPTS, 4). 5-FU (0.2 mmol, 26 mg) was dissolved in MeOH, and a methanolic solution of KOH was then added (0.2 mmol). The solution was left reacting for 10 minutes, and then, [AuCl(PR$_3$)] (0.2 mmol) was added to the solution. After 1 hour of reaction, the solvent was evaporated to minimum volume under vacuum and a precipitate was obtained by the addition of Et_2O. The solid was filtered, washed with diethyl ether, and dried.

[Au(5-FU)(PTA)] (1). [Au(5-FU)(PTA)] was obtained in 98% yield as an off-white powder. ^{1}H NMR (400 MHz, DMSO-d_6, 25 °C): δ = 10.33 (br s, 1H, NH), 7.51 (br s, 1H, H_{5FU}^{6}), 4.55 and 4.37 (AB system, J_{AB} = 12.0 Hz, 6H, NCH_2N), 4.35 (s, 6H, NCH_2P) ppm. ^{31}P{^{1}H} NMR (162 MHz, DMSO-d_6, 25 °C): δ = −57.1 ppm. ^{13}C{^{1}H} NMR (101 Hz, 25 °C): δ = 160.8 (br s, 1C, C_{5FU}^{4}), 155.2 (s, 1C, C_{5FU}^{2}), 141.8 (d, J = 223.1 Hz, 1C, C_{5FU}^{5}), 129.7 (br s, 1C, C_{5FU}^{6}), 71.8 (d, J = 8.4 Hz, 3C, NCH_2N), 50.7 (d, J = 23.2 Hz, 3C, NCH_2P) ppm. ^{19}F{^{1}H} NMR (376.52 MHz, 25 °C): δ = −169.4 (s, 1F) ppm. IR ν_{max}/cm^{-1}: 1636, 1587 (CO). MALDI MS m/z (%): 484.05 (14) $[M + H]^+$, 511.16 (100) $[Au(PTA)_2]^+$, 455.43 (13) $[Au(5\text{-}FU)_2 + H]^+$, 837.08 (5) $[M + AuPTA]^+$. Anal. calcd (%) for $C_{10}H_{14}AuFN_5O_2P$ (483.19): C, 24.86; H, 2.92; N, 14.49. Found: C, 24.85; H, 2.56; N, 14.32.

[Au(5-FU)(DAPTA)] (2). [Au(5-FU)(DAPTA)] was obtained in 58% yield as an off-white powder. ^{1}H NMR (300 MHz, DMSO-d_6, 25 °C): δ = 7.98 (br s, 1H, NH), 7.50 (d, J = 5.5 Hz, 1H, H_{5FU}^{6}), 5.51 (d, J = 13.5 Hz, 1H, NCH_2N), 5.39 (dd, J = 15.1, 9.8 Hz, 1H, NCH_2P), 4.92 (d, J = 13.5 Hz, 1H, NCH_2N), 4.84 (d, J = 11.6 Hz, 1H, NCH_2P), 4.65 (d, J = 13.5 Hz, 1H, NCH_2N), 4.31 (d, J = 15.5 Hz, 1H, NCH_2P), 4.13 (d, J = 13.5 Hz, 1H, NCH_2N), 4.04 (s, 2H, NCH_2P), 3.78 (d, J = 15.1 Hz, 1H, NCH_2P), 1.98 (s, 3H, CH_3), 1.96 (s, 3H, CH_3) ppm. ^{31}P{^{1}H} NMR (162 MHz, 25 °C): δ = −30.9 (s, 1P, DAPTA) ppm. ^{13}C{^{1}H} NMR (101 MHz, 25 °C): δ = 169.4 (s, 1C, CO-DAPTA), 168.6 (s, 1C, CO-DAPTA), 157.0 (br s, 1C, C_{5FU}^{4}), 66.5 (d, J = 5.6 Hz, 1C, NCH_2N), 61.0 (d, J = 5.6 Hz, 1C, NCH_2N), 47.3 (d, J = 28.3 Hz, 1C, NCH_2P), 43.7 (d, J = 29.1 Hz, 1C, NCH_2P), 38.2 (d, J = 30.2 Hz, 1C, NCH_2P), 21.5 (s, 1C, CH_3), 21.2 (s, 1C, CH_3) ppm. ^{19}F{^{1}H} NMR (282 MHz, 25 °C): δ = −170.9 (s, 1F) ppm. IR ν_{max}/cm^{-1}: 1630, 1585 (CO). MALDI MS m/z (%): 556.13 (6) $[M + H]^+$, 594.09 (69) $[M + K]^+$, 655.23 (100) $[Au(DAPTA)_2]^+$, 365.2 (39) $[Au(5\text{-}FU) + K]^+$. Anal. calcd (%) for $C_{13}H_{18}AuFN_5O_4P$ (555.26): C, 28.12; H, 3.27; N, 12.61. Found: C, 28.47; H, 3.43; N, 12.72.

[Au(5-FU)(PPh$_3$)] (3). [Au(5-FU)(PPh$_3$)] was obtained in 50% yield as an off-white powder. ^{1}H NMR (400 MHz, DMSO-d_6, 25 °C): 7.67–7.56 (m, 15H, PPh_3), 7.54 (d, J = 5.4 Hz, 1H, H_{5FU}) ppm. ^{31}P{^{1}H} NMR (162 MHz): δ = 31.6 ppm. ^{19}F{^{1}H} NMR (376.52 MHz): δ = −169.41 ppm. ^{13}C{^{1}H} NMR (101 MHz, 25 °C): δ = 156.5 (s, br, $C_{5FU}^{2,4}$), 141.2 (d, J = 227.3 Hz, 1C, C_{5FU}^{5}), 133.9 (d, 6C, J = 13.7 Hz, PPh_3), 132.3 (s, 3C, PPh_3), 129.7 (d, J = 11.6 Hz, 6C, PPh_3), 128.6 (d, J = 61.7 Hz, C_{ipso}, 3C, PPh_3) ppm. IR ν_{max}/cm^{-1}: 1621, 1590 (CO). MALDI MS m/z (%): 236.037 (9) $[M - PPh_3]^+$, 589.02 (1) $[M]^+$, 459.051 (80) $[Au(PPh_3)]^+$, 721.104 (100) $[Au(PPh_3)_2]^+$. Anal. calcd (%) for $C_{22}H_{17}AuFN_2O_2P$ (588.33): C, 44.91; H, 2.91; N, 4.76. Found: C, 44.45; H, 2.65; N, 4.33.

[Au(5-FU)(TPPTS)] (4). [Au(5-FU)(TPPTS)] was obtained in 87% yield as an off-white powder. ^{1}H NMR (400 MHz, DMSO-d_6, 25 °C): δ = 7.93–7.83 (m, 6H, Ph), 7.64–7.61 (m, 4H, Ph + H_{5FU}^{6}), 7.51–7.46 (m, 3H, Ph) ppm. ^{31}P {^{1}H} (162 MHz, DMSO): δ = 32.3 ppm. ^{19}F {^{1}H} (376.52 MHz, DMSO): δ = −169.57 ppm. ^{13}C{^{1}H} NMR (101 MHz, 25 °C): δ = 155.1 (s, br, $C_{5FU}^{2,4}$), 149.1 (d, J = 10.1 Hz, 3C, TPPTS), 133.8 (d, 3C, J = 12.2 Hz, 6C, TPPTS), 130.8 (d, J = 16.4 Hz, TPPTS), 129.7 (s, 3C, TPPTS), 129.6 (s, 3C, TPPTS), 127.9 (d, J = 60.5 Hz, C_{ipso}, TPPTS) ppm. IR ν_{max}/cm^{-1}: 1149, 1097 (SO); 1651, 1599 (C═O). MALDI MS m/z (%): 236.367 (23) $[M - TPPTS]^+$. Anal. calcd (%) for $C_{22}H_{14}AuFN_2Na_3O_{11}PS_3$ (894.445): C, 29.54; H, 1.58; N, 3.13. Found: C, 29.15; H, 1.51; N, 2.91.

[Au$_2$(5-FU)(PTA)$_2$] (5). [Au_2(5-FU)$(PTA)_2$] was obtained in 86% yield as an off-white powder. ^{1}H NMR (400 MHz, D_2O, 25 °C): δ = 7.76 (br s, 1H, H_{5FU}^{6}), 4.70–4.55 (m, 12H, NCH_2N), 4.40 (s, 6H, NCH_2P), 4.37 (s, 6H, NCH_2P) ppm. ^{31}P{^{1}H} NMR (162 MHz, 25 °C): δ = −51.9 (s, 1P, PTA), −52.7 (s, 1P, PTA) ppm. ^{13}C{^{1}H} NMR (101 Hz, 25 °C): δ = 70.9 (s, 12C, NCH_2N), 49.8 (s, 3C, NCH_2P), 49.7 (d, J = 25.2 Hz, 3C, NCH_2P) ppm. ^{19}F {^{1}H} NMR (376.52 MHz, D_2O, 25 °C): δ = −169.2 (s, 1F) ppm. IR ν_{max}/cm^{-1}: 1534, 1443 (CO). MALDI MS m/z (%): 837.2 (3) $[M + H]^+$, 511.16 (100) $[Au(PTA)_2]^+$, 847.19 (50) $[M - CO + K]^+$. Anal. calcd (%) for $C_{16}H_{25}Au_2FN_8O_2P_2$ (836.31): C, 22.98; H, 3.01; N, 13.40. Found: C, 22.54; H, 3.22; N, 13.64.

Solution chemistry

Stability in solution assay. The stability of the gold complexes in solution was analysed by UV-vis absorption spectroscopy. UV-vis absorption spectra of the complexes were recorded on a Thermo Scientific Evolution 600 spectrophotometer. First, stock solutions of the new complexes were prepared at 10 mM in DMSO. From these, working solutions (10 mL) were prepared at 50 μM in PBS at pH = 7.4. The samples were then incubated at 37 °C and thereafter monitored by measuring the electronic spectra over 24 h.

Stability in solution in the presence of a reducing agent/NAC-ME. ^{1}H NMR spectra were recorded in a mixture of DMSO-d_6 : D_2O (80 : 20) containing the gold complexes (0.03 mmol) with an equimolecular amount of *N*-acetyl cysteine methyl ester (NAC-ME). The corresponding NMR spectra were recorded immediately after preparation, at time 0 and after 24 h.

 This journal is © The Royal Society of Chemistry 2023

Open Access Article. Published on 30 June 2023. Downloaded on 6/13/2026 6:36:53 AM. This article is licensed under a Creative Commons Attribution-NonCommercial 3.0 Unported Licence.

Bacterial proliferation assays

The bacterial strains used, *Bacillus subtilis* (Ehrenberg 1835) Cohn 1872 – CECT 35 and *Escherichia coli* (Migula 1895) Castellani and Chalmers 1919 – CECT 101, were acquired from the Colección Española de Cultivos Tipo (CECT) as lyophilized bacteria. The bacterial cell bank suspensions were thawed and inoculated on an agar plate and on a liquid medium (nutrient broth – NB – for *B. subtilis* and LB (Miller) broth – LB – for *E. coli*) at 37 °C for 24 h with mild agitation. A first subculture was performed to assure the viability of the strain. A dilution from these culture solutions (second subculture and so on) was used for the following tests, corresponding to an inoculum of 10^7 CFU mL^{-1}. Considering that the dilution to the well will be 1 : 100, stock solutions were prepared – in DMSO – ×100 more concentrated than the final concentration in the well (409.6 mg mL^{-1}, 204.8 mg mL^{-1}, 102.4 mg mL^{-1}, and so on).

Bacterial growth inhibition assay (MIC). First, 98 μL of the appropriate liquid media and 2 μL of the compound at the corresponding concentration required for the assay were added per well to a 96-well plate. Then, 100 μL of the 10^7 CFU mL^{-1} inoculum was added per well. Bacterial growth at 37 °C was controlled by visual observation of the turbidity in each well and confirmed by optical density at 600 nm at time points 0 h and 24 h. Results (MIC) were recorded as the lowest concentration of antimicrobial agent that inhibits visible growth of the bacteria and were compared with the variation of a control culture containing *E. coli* or *B. subtilis* (positive control) and of solution of the tested compounds without bacteria as well as only culture medium (negative control).

Bacterial cell viability assay (MBC). Cell viability was analysed using a resazurin (7-hydroxy-3*H*-phenoxazin-3-one 10-oxide) assay in a 96-well plate. Once the bacterial cultures of the growth inhibition assay had been grown for a total of 24 h, 25 μL of 0.1 mg mL^{-1} resazurin (prepared in LB medium) was added to each well and incubated in the dark at 37 °C for 1 h under stirring. Resazurin has a blue colour at the testing pH and turns pink when reduced by the viable bacteria to resorufin. Therefore, pink wells indicate metabolizing bacteria, while blue wells are indicative of bacteria that have lost their ability to convert resazurin to resorufin. The viability of bacteria was verified (either confirmed or rejected) by the colony plate-counting method, by seeding 10 μL from the cell culture onto NB agar plates and observing the presence or absence of bacterial growth following incubation at 37 °C for 24 h.

Preparation of bacteria for scanning electron microscopy

In a 24-well plate, 500 μL of bacteria culture (10^7 CFU mL^{-1}) was added per well and was treated with 5-FU, **1** and **5** at their corresponding MIC and 1/2× MIC. A positive control of bacteria without any treatment and a negative control of only culture medium were included, following the same protocol. Once the plates were prepared, bacteria were incubated at 37 °C for 24 h with mild agitation. After this time, bacterial suspensions were transferred into 1.5 mL centrifugation tubes for fixation and were centrifuged at 3000 rpm for 15 minutes. The pellet was washed twice with sterile PBS and then resuspended in 1.5 mL of a 2.5% glutaraldehyde solution in 10 mM PBS with pH 7.2. The suspensions were incubated in a tube rotator for 2 hours. Next, bacteria were washed with PBS (×1) and ultrapure H_2O (×3). The fixed bacteria were then washed with PBS (×3) and dehydrated with increasing concentrations of EtOH (30%, 50%, 70%, 90%, 96%, and 100%) for 10 minutes each. Finally, 10 μL of the suspensions were transferred onto silicon wafer squares, allowed to dry and then coated with 14 nm of carbon.

Results and discussion

Synthesis and characterisation of gold complexes

Deprotonation of 5-FU with KOH in methanol, followed by the addition of [AuCl(PR$_3$)] (PR$_3$ = PTA, DAPTA, PPh$_3$ and TPPTS) afforded the corresponding mononuclear derivatives [Au(5-FU)(PR$_3$)] (PR$_3$ = PTA, **1**; DAPTA, **2**; PPh$_3$, **3** and TPPTS, **4**) (Scheme 1) as off-white air-stable solids.

In the ^{1}H NMR spectra of the new derivatives, the signal corresponding to the pyrimidine proton at position 6 is observed at around 7.50 ppm, as a doublet in the case of complex **2** with a J_{H-F} of 5.5 Hz, which implies an up-field shift compared to that of free 5-FU (7.75 ppm). In the case of the PTA complexes (**1** and **5**) and the TPPTS complex (**4**), the signal appears as a broad signal, and in the PPh$_3$ derivative (**3**), the signal appears together with the multiplet due to PPh$_3$. The signal of an N–H proton is only clearly detected in the cases of PTA and DAPTA derivatives, as a broad singlet centred at 10.3 ppm for [Au(5-FU)(PTA)] (**1**) and at 7.98 ppm for the DAPTA analogue. It is not possible to distinguish between the coordination to the nitrogen atoms N1 and N3 with the available NMR data. Deprotonation of either N1 or N3 is very dependent on the solvent used in the reaction, as different solvents stabilize the different anions involved in deprotonation. Thus, deprotonation of the nitrogen at position N1 occurs in DMSO as solvent, while anions at both nitrogen positions are formed in an aqueous alkaline solution; in addition, more polar solvents stabilize the formation of the corresponding N3 anion.[45,46] Since the reactions have been carried out in methanol, a solvent with an intermediate polarity between that of

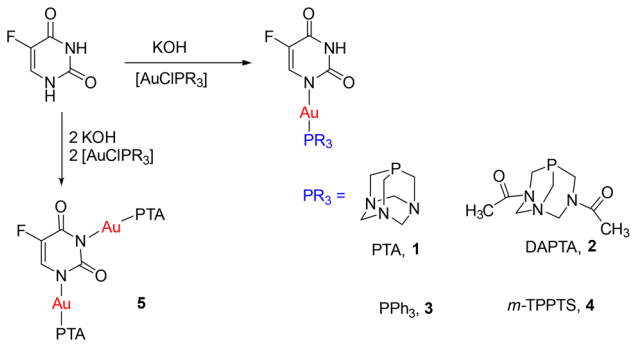

Scheme 1 Synthesis of 5-FU gold(I) derivatives, **1–5**.

Open Access Article. Published on 30 June 2023. Downloaded on 6/13/2026 6:36:53 AM. This article is licensed under a Creative Commons Attribution-NonCommercial 3.0 Unported Licence.

DMSO and water, the deprotonation and subsequent gold coordination could happen at both nitrogen positions. Besides, methylene protons of the PTA and DAPTA fragment integration with respect to the pyrimidine H(6) proton, confirming the 5-FU : PTA ratios of 1 : 1 for both complexes, which is also measured in the TPPTS derivative (integration of Ph and H(6) signals).

The $^{31}P\{^{1}H\}$ NMR spectra in DMSO-d_6 at room temperature display a singlet in all the complexes. In the case of [Au(5-FU)(PTA)] (**1**), the spectrum in D_2O shows a singlet at −51.6 ppm and a small signal at −52.3 ppm, which could indicate a fast interchange of the coordination position between N1 and N3 atoms of the pyrimidine moiety. Accordingly, NMR experiments have been performed at low temperatures in MeOD only in the case of complex [Au(5-FU)(DAPTA)] (**2**), which showed enough solubility in MeOD even at below 0 °C. Therefore, the $^{31}P\{^{1}H\}$ NMR spectrum of **2** at 213 K exhibits the formation of two signals at −23.7 and −27.8 ppm (Fig. 1), which appeared as a singlet at room temperature. The resolution of two singlets at low temperatures could be indicative of gold coordination to both nitrogen atoms after being deprotonated in methanol, as mentioned above, or to the formation of the two isomers in solution.

According to Abdrakhimova *et al.*,[46] C6 resonance is more strongly deshielded in the $^{13}C\{^{1}H\}$ NMR spectra of the derivatives compared to 5-FU, which is in agreement with the coordination of the metallic centre to the N1 atom, a consequence of deprotonation of the N1 atom in 5-FU.

The addition of two equivalents of KOH and the corresponding chloro-gold phosphine to 5-FU afforded the dinuclear derivative only in the case of PTA [Au_2(5-FU)$(PTA)_2$] (**5**), probably due to the higher spatial requirement of DAPTA, PPh_3 and TPPTS, which are bulkier than PTA,[47–49] resulting in stronger steric hindrance and making the coordination of two $AuPR_3$ moieties more difficult. The signal of the N–H proton is not observed in the ^{1}H NMR spectrum of **5**, confirming the deprotonation of both nitrogen atoms and the coordination of both Au-PTA units. Methylene protons of the PTA fragment integration in a 24 : 1 relationship with respect to the pyrimidine H(6) proton, confirming the 5-FU : PTA ratio of 1 : 2. Besides, these signals are slightly more complicated than those observed in the mononuclear [Au(5-FU)(PTA)] (**1**), as the signals of the methylene protons of NCH_2N overlap in a multiplet between 4.66 and 4.51 ppm, and methylene protons in the NCH_2P moiety are seen as two singlets at 4.36 and 4.32 ppm, indicating that the two different Au-PTA fragments are inequivalent, as their chemical environment is not the same. This inequivalence can also be detected in the $^{31}P\{^{1}H\}$ NMR spectrum, where two singlets are observed at −51.9 and −52.7 ppm, with a ratio of 1 : 1, meaning that both phosphorus atoms are linked to Au in a similar manner, although in a different environment.

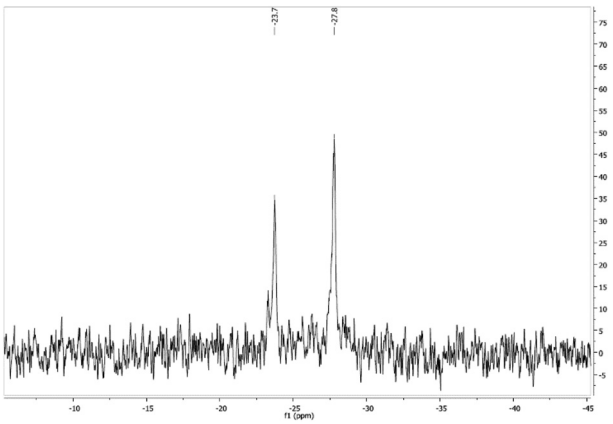

Fig. 1 $^{31}P\{^{1}H\}$ NMR spectrum of [Au(5-FU)(DAPTA)] (**2**) in MeOD at 213 K.

Experimental and calculated absorption spectra of 5-FU, and its different anions and tautomers, have been widely studied by Raman spectroscopy[45,50] and IR spectroscopy.[38,51,52] In the case of 5-FU, a group of complex and strong absorption bands for the carbonyl groups appear in the range from 1720 to 1650 cm^{-1}, together with the C–H absorption band (Fig. S11†). Upon coordination of gold to the nitrogen atoms, these bands decrease in intensity and appear shifted to lower frequencies: 1636 and 1587 cm^{-1} for **1**, 1534 and 1443 cm^{-1} for **2**, 1651 and 1599 cm^{-1} for **3**, 1588 and 1619 cm^{-1} for **4** and 1630 and 1585 cm^{-1} for **5**. This shift indicates a reduction of the double-bond character of C=O by the coordination of gold so that the pair of electrons of the carbonyl group move to favour a nitrogen–Au(I) bond, as has been stated in other examples of N–M coordination in 5-FU complexes[38,53] and also in the study of the formation of 5-FU anions and dianions.[52] Furthermore, the numerous N–H bands observed in the spectrum of 5-FU decrease in number and intensity in the case of the mononuclear derivatives **1**–**4**, disappearing in the spectrum of dinuclear complex **5**. Unfortunately, no single crystals were obtained for any of the complexes to confirm the structure in the solid state. The low solubility of these compounds in any solvent suitable for single crystal growth hinders the formation of crystals suitable for X-ray diffraction.

Stability of gold complexes in solution

The stability of the new complexes was analysed by UV-vis absorption spectroscopy in PBS solution (pH = 7.4). 5×10^{-5} M solutions were prepared by diluting DMSO stock solutions of the complexes in PBS buffered at pH 7.4. The resulting solutions were monitored over 24 h at 37 °C. The spectra of the complexes (Fig. S12†) show an absorption band with low intensity at around 260 nm, which could be assigned to $\pi \rightarrow \pi^*$ intra-ligand transitions. These bands remain without any changes in shape and non-apparent red or blue shifts are observed in all the new derivatives, in addition to a lack of absorbance at around 500 nm over 24 h, which is characteristic of gold nanoparticle formation, implying substantial stability of the chromophore under physiological conditions. Changes in the baseline intensity for complexes **1**, **3** and **5** are due to low solubility in PBS preventing a homogeneous solution being obtained at the studied concentration.

Besides, the reactivity of the complexes towards model nucleophiles was studied by mixing them with *N*-acetyl

 This journal is © The Royal Society of Chemistry 2023

Open Access Article. Published on 30 June 2023. Downloaded on 6/13/2026 6:36:53 AM. This article is licensed under a Creative Commons Attribution-NonCommercial 3.0 Unported Licence.

cysteine methyl ester (NAC-ME) in equimolecular amounts.[54] The resulting solutions were analysed by ^{1}H NMR over time (Fig. S13†). NAC-ME underwent auto-oxidation, displaying new signals at around 3, 1.8 and 4.4 ppm after 24 h, as a consequence of sulphur bridge formation. All the complexes seemed to be inert with respect to ligand exchange reactions with this nucleophile, since no new signals were detected apart from those obtained from the auto-oxidation of NAC. Moreover, the solution did not change colour, indicating that there was no reduction of Au(III) to Au(0), confirming the high stability of the complexes.

Antibacterial activity of the gold(I)–5-FU complexes

As previously mentioned, 5-FU has shown antibacterial activity against different bacterial strains, both Gram-negative and Gram-positive. Its activity arises mostly from the suppression of virulence genes and actions, quenching quorum-sensing in bacteria and preventing the formation of biofilms.[12,55,56] In this study, we have found 5-FU to be more active against Gram-positive *B. subtilis* than against Gram-negative *E. coli* (Table 1). In general, all the compounds presented higher antibacterial activity than 5-fluorouracil alone, confirming the fact that the incorporation of a metallic centre improves this activity, as previously observed for a silver(I) complex with 5-FU.[33] Furthermore, the antibacterial activity of these gold(I) complexes against *B. subtilis* and *E. coli* is in the same range shown by auranofin and its derivatives of similar structure. It has been shown that the mechanism of action of auranofin against Gram-positive bacteria arises from the inhibition of TrxR after the coordination of the Au–phosphine unit to its cysteine residues.[21,29]

With the exceptions of compound **3** for *E. coli* and compound **4** for *B. subtilis*, the addition of gold–phosphane units to 5-FU increased the inhibitory activity up to ×64. All complexes possessed bactericidal activity, with MBC/MIC ratios lower than 4 in all cases. Complexes **1** and **5** show the highest activity against both strains. The improvement of the activity is even stronger when comparing the MIC and MBC values in nM instead of μg mL^{-1} (Table S1†).

Gram-negative bacteria have a more complex and robust cell wall and a highly developed efflux-mediated resistance mechanism, which confers them with greater resistance capacity against antibiotics. Multi-drug resistant Gram-negative bacteria are of special concern and great research effort must be put into developing new effective antibiotics. In general, 5-FU and its Au(I) complexes are more active against the Gram-positive *B. subtilis* than against the Gram-negative *E. coli*, as has been previously observed for metallic complexes and antibiotics in general.[57]

Nevertheless, it is interesting to observe differences in the activity of the complexes depending on the size and hydrophobicity of their phosphane ligands – which could be extrapolated to the complex. Complex **3**, which has the most hydrophobic phosphane, PPh_3, presents the lowest antibacterial activity against *E. coli* but in turn, it is the most active against *B. subtilis*. On the other hand, complex **1** is the most bactericidal complex against *E. coli*, with a non-insignificant MBC value of 64 μg mL^{-1}. Based on these results, higher hydrophilicity and smaller size improve the bactericidal activity of the complexes against the Gram-negative model bacteria *E. coli*. This has been previously observed for gold complexes, improving their activity against Gram-negative bacteria with the use of smaller alkylphosphines.[28,58] Given these results, it would be interesting to further study the size and hydrophilicity of gold complexes to increase their bactericidal activity against Gram-negative bacteria.

Gold(I)–phosphine complexes are in general mainly effective against Gram-positive bacteria and inactive in most of the cases against Gram-negative bacteria. In our case, all complexes enhance the activity of 5-fluorouracil against Gram-positive bacteria except for complex **4**. Furthermore, all of them inhibit the growth of *E. coli* bacteria (Gram-negative) more effectively than 5-FU, except for the complex with PPh_3, similar to the starting material [AuClPPh$_3$].[59] This fact suggests that the presence of the gold–phosphine unit is essential to induce an increase in the activity of the final complexes.

Besides, examples are known of complexes with the N–Au–phosphine core,[60,61] as in our case, that inhibit the growth of Gram-negative bacteria, most likely because of their capacity to interact with the membrane or specific biomolecules present in the membrane.

Electron microscopy is a useful method for the observation of bacteria and the impact on their growth and death caused by antimicrobial agents. Here we used scanning electron microscopy (SEM) to further examine the effect of 5-FU and the complexes **1**, **3** and **5** on *E. coli* and *B. subtilis* (Fig. 2). Bacteria were incubated for 24 h without any treatment or in the presence of the different compounds at concentrations corresponding to their MIC values. Since the MIC value for complex **3** against *E. coli* was not found at the tested concentrations, the highest concentration tested (1024 μg mL^{-1}) was used for the incubation. In *E. coli*, the effect of complexes **1** and **5** can be observed in the cell since the surface of the bacteria loses its smooth appearance with the presence of dents and depressions. Incubation with 5-FU affects some of the bacteria in the samples, with changes in morphology and the membrane. Meanwhile, complex **3** does not have an observable effect compared to the control, at least observable in SEM.

Table 1 Minimum inhibitory concentration (MIC) and minimum bactericidal concentration (MBC), in μg mL^{-1}, of the different compounds against Gram-negative *Escherichia coli* and Gram-positive *Bacillus subtilis*

	E. coli		*B. subtilis*	
Compound	MIC	MBC	MIC	MBC
5-FU	1024	>1024	64	128
1	32	64	8	16
2	64	128	16	32
3	>1024	>1024	1	1
4	256	512	64	128
5	128	128	2	4

Open Access Article. Published on 30 June 2023. Downloaded on 6/13/2026 6:36:53 AM.
This article is licensed under a Creative Commons Attribution-NonCommercial 3.0 Unported Licence.

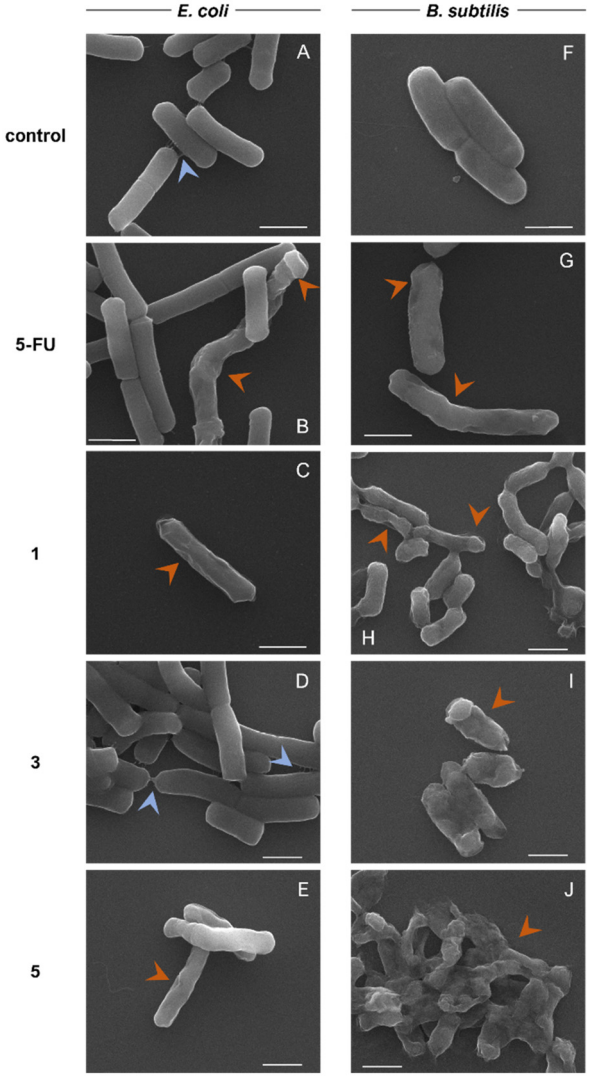

Fig. 2 Scanning electron microscopy (SEM) images of *E. coli* (A–E) and *B. subtilis* (F–J) without treatment (control, A & F) and after incubation with 5-FU (B & G) or complexes **1** (C & H), **3** (D & I) and **5** (E & J), at their corresponding MIC (50k×–60k×) and at the highest tested concentration (1024 μg mL^{-1}) in the case of complex **3** for *E. coli*. Scale bar = 1 μm. Orange arrows indicate cell damage, while blue arrows indicate biofilm matrix formation.

The limited ability to combat Gram-negative strains in the case of most of the inactive gold complexes is potentially linked to a decreased uptake of the drug caused by the permeability of the outer membrane barrier.[62] In fact, modification of the ligands of auranofin can modulate the antimicrobial activity rendering effective complexes even against Gram-negative strains.[28] In our case, the damage on the surface of the cell membrane observed by SEM studies could be indicative of an enhanced activity and higher interaction with the bacterial membrane.

Furthermore, an extracellular biofilm matrix can be seen in the control of *E. coli* and in the incubation with complex **3** attaching to several cells (Fig. 2, light blue arrows), while it is not observed in the presence of 5-FU or complexes **1** and **5**. The biofilm matrix is produced by bacteria and is mainly composed of polysaccharides, proteins and extracellular DNA. It confers great protection to the bacteria within the biofilm, as well as adherence to the surface, and is thought to be key for the development of antibiotic resistance and virulence. It has been previously described that 5-FU reduces the formation of biofilms in different strains of *E. coli* in a dose-dependent manner.[63] This inhibitory effect could be maintained in the case of the active Au(I) complexes. The effect of the metallic complexes is more evident in the case of *B. subtilis*. After treatment with 5-FU, the surface of the bacteria appears damaged, while complexes **1**, **3** and **5** clearly produce not only disruption of the bacterial cell wall but also changes in morphology such as compression and accumulation of intracellular material at the extremes of the bacteria. In the sample of *B. subtilis* treated with complex **5**, a mass of material surrounding the bacteria could be observed. Analysis of the sample by detection of backscattered electrons indicates the possible presence of gold in the mass, which is further confirmed by energy dispersive X-ray spectroscopy (Fig. S14†).

Conclusions

Here, we report the synthesis of new gold(I) phosphane complexes of 5-fluorouracil, an analogue of the nucleobase uracil used for the treatment of different types of cancer, including the first example of a dinuclear gold(I) complex. All the compounds demonstrated good stability under simulated physiological conditions in solution, even in the presence of *N*-acetylcysteine methyl ester (NAC-ME). Their activity as antibacterial agents was evaluated against two model bacterial strains: *E. coli* and *B. subtilis*. While 5-FU was shown to be the principal bactericidal agent, the introduction of the metallic centre improved the activity of the complexes, compared to 5-FU on its own. This is especially relevant in the case of the dinuclear complex, which demonstrated excellent activity against *B. subtilis*. Furthermore, the interaction of the compounds with bacteria was studied by scanning electron microscopy, and damage to the membrane could be observed after incubation with the tested compounds. This study offers new ways to complex known drugs with metallic centres offering a route to combined therapies as a method to increase their bioactivity and potentially combat the resistance generated in microorganisms and cancerous cells. Future work will focus on how fine tuning the chemistry, *e.g.*, optimising the size and hydrophilicity of the complexes, can affect more specifically the additive or synergic activity of such gold(I)–fluorouracil complexes against a wider spectrum of bacteria.

Conflicts of interest

There are no conflicts to declare.

This journal is © The Royal Society of Chemistry 2023

Open Access Article. Published on 30 June 2023. Downloaded on 6/13/2026 6:36:53 AM. This article is licensed under a Creative Commons Attribution-NonCommercial 3.0 Unported Licence.

Acknowledgements

This work was financially supported by MCIN-Agencia Estatal de Investigación Grants PID2019-104379RB-C21/AEI/10.13039/501100011033, and Red Multimetdrugs (RED2018-102471-T/MCIN/AEI/10.13039/501100011033) and Gobierno de Aragón (E07_20R, Fondos FEDER "otra manera de hacer Europa"). E. A. B. and S. G. M. acknowledge the funding from the European Union's Horizon 2020 research and innovation program (Marie Skłodowska-Curie grant agreement no. 845427) and from the internationalization program "MSCA-IF_ERC" of CSIC. The authors acknowledge Servicio General de Apoyo a la Investigación-SAI (Universidad de Zaragoza) and the use of instrumentation as well as the technical advice provided by the National Facility ELECMI ICTS, node "Laboratorio de Microscopías Avanzadas" at the University of Zaragoza.

References

1 C. Heidelberger, N. K. Chaudhuri, P. Danneberg, D. Mooren, L. Griesbach, R. Duschinsky, R. J. Schnitzer, E. Pleven and J. Scheiner, *Nature*, 1957, **179**, 663–666.
2 J. A. Meyerhardt and R. J. Mayer, *N. Engl. J. Med.*, 2005, **352**, 476–487.
3 D. Cunningham, W. Atkin, H. J. Lenz, H. T. Lynch, B. Minsky, B. Nordlinger and N. Starling, *Lancet*, 2010, **375**, 1030–1047.
4 C. Tournigand, T. Andre, F. Bonnetain, B. Chibaudel, G. Lledo, T. Hickish, J. Tabernero, C. Boni, J.-B. Bachet, L. Teixeira and A. de Gramont, *J. Clin. Oncol.*, 2012, **30**, 3353–3360.
5 T. Andre, C. Boni, L. Mounedji-Boudiaf, M. Navarro, J. Tabernero, T. Hickish, C. Topham, M. Zaninelli, P. Clingan, J. Bridgewater, I. Tabah-Fisch and A. de Gramont, *N. Engl. J. Med.*, 2004, 2343–2351.
6 D. B. Longley, D. P. Harkin and P. G. Johnston, *Nat. Rev. Cancer*, 2003, **3**, 330–338.
7 R. I. Ceilley, *J. Dermatol. Treat.*, 2012, **23**, 83–89.
8 J. M. Thomson and I. L. Lamont, *Front. Microbiol.*, 2019, **10**, 952.
9 C. Oe, H. Hayashi, K. Hirata, K. Kawaji, F. Hashima, M. Sasano, M. Furuichi, E. Usui, M. Katsumi, Y. Suzuki, C. Nakajima, M. Kaku and E. N. Kodama, *ACS Infect. Dis.*, 2020, **6**, 1490–1500.
10 A. Ueda, C. Attila, M. Whiteley and T. K. Wood, *Microb. Biotechnol.*, 2009, **2**, 62–74.
11 C. Attila, A. Ueda and T. K. Wood, *Appl. Microbiol. Biotechnol.*, 2009, **82**, 525–533.
12 A. Rangel-Vega, L. Bernstein, E. A. Mandujano-Tinoco, S. J. García-Contreras and R. García-Contreras, *Front. Microbiol.*, 2015, **6**, 282.
13 E. R. T. Tieknik, *Crit. Rev. Oncog.*, 2002, **42**, 225.
14 B. D. Glisic and M. I. Djuran, *Dalton Trans.*, 2014, **43**, 5950–5969.
15 J. R. Stenger-Smith and P. K. Mascharak, *ChemMedChem*, 2020, **15**, 2136–2145.
16 F. Novelli, M. Recine, F. Sparatore and C. Juliano, *Farmaco*, 1999, **54**, 232–236.
17 R. Visbal and M. C. Gimeno, *Chem. Soc. Rev.*, 2014, **43**, 3551–3574.
18 A. AbdelKhalek, N. S. Abutaleb, H. Mohammad and M. N. Seleem, *Int. J. Antimicrob. Agents*, 2019, **53**, 54–62.
19 L. Aguinagalde, R. Diez-Martinez, J. Yuste, I. Royo, C. Gil, I. Lasa, M. Martin-Fontecha, N. I. Marin-Ramos, C. Ardanuy, J. Linares, P. Garcia, E. Garcia and J. M. Sanchez-Puelles, *J. Antimicrob. Chemother.*, 2015, **70**, 2608–2617.
20 T. Marzo, D. Cirri, S. Pollini, M. Prato, S. Fallani, M. I. Cassetta, A. Novelli, G. M. Rossolini and L. Messori, *ChemMedChem*, 2018, **13**, 2448–2454.
21 J. P. Owings, N. N. McNair, Y. F. Mui, T. N. Gustafsson, A. Holmgren, M. Contel, J. B. Goldberg and J. R. Mead, *FEMS Microbiol. Lett.*, 2016, **363**, fnw148.
22 N. S. Abutaleb and M. N. Seleem, *Int. J. Antimicrob. Agents*, 2020, **55**, 105828.
23 A. N. Kuntz, E. Davioud-Charvet, A. A. Sayed, L. L. Califf, J. Dessolin, E. S. J. Arner and D. L. Williams, *PLoS Med.*, 2007, **4**, 1071–1086.
24 M. Bonilla, A. Denicola, S. V. Novoselov, A. A. Turanov, A. Protasio, D. Izmendi, V. N. Gladyshev and G. Salinas, *J. Biol. Chem.*, 2008, **283**, 17898–17907.
25 A. R. Sannella, A. Casini, C. Gabbiani, L. Messori, A. R. Bilia, F. F. Vincieri, G. Majori and C. Severini, *FEBS Lett.*, 2008, **582**, 844–847.
26 A. Ilari, P. Baiocco, L. Messori, A. Fiorillo, A. Boffi, M. Gramiccia, T. Di Muccio and G. Colotti, *Amino Acids*, 2012, **42**, 803–811.
27 N. Tejman-Yarden, Y. Miyamoto, D. Leitsch, J. Santini, A. Debnath, J. Gut, J. H. McKerrow, S. L. Reed and L. Eckmann, *Antimicrob. Agents Chemother.*, 2013, **57**, 2029–2035.
28 B. Wu, X. J. Yang and M. D. Yan, *J. Med. Chem.*, 2019, **62**, 7751–7768.
29 M. B. Harbut, C. Vilcheze, X. Z. Luo, M. E. Hensler, H. Guo, B. Y. Yang, A. K. Chatterjee, V. Nizet, W. R. Jacobs, P. G. Schultz and F. Wang, *Proc. Natl. Acad. Sci. U. S. A.*, 2015, **112**, 4453–4458.
30 M. F. Mogilevkina and V. A. Shipachev, *Koord. Khim.*, 1994, **20**, 51–53.
31 X. Y. Wang, J. Lin, X. M. Zhang, Q. Liu, Q. Xu, R. X. Tan and Z. J. Guo, *J. Inorg. Biochem.*, 2003, **94**, 186–192.
32 M. F. Mogilevkina, V. A. Shipachev, G. P. Troshkova, M. A. Mazurkova, M. P. Martynets and M. P. Bagryantseva, *Pharm. Chem. J.*, 1999, **33**, 68–70.
33 J. H. B. Nunes, F. R. G. Bergamini, W. R. Lustri, P. P. de Paiva, A. L. T. G. Ruiz, J. E. de Carvalho and P. P. Corbi, *J. Fluor. Chem.*, 2017, **195**, 93–101.
34 M. Barceló-Oliver, B. A. Baquero, A. Bauzá, Á. García-Raso, R. Vich, I. Mata, E. Molins, À. Terrón and A. Frontera, *Dalton Trans.*, 2013, **42**, 7631–7642.

Open Access Article. Published on 30 June 2023. Downloaded on 6/13/2026 6:36:53 AM. This article is licensed under a Creative Commons Attribution-NonCommercial 3.0 Unported Licence.

35 I. Okamoto, K. Iwamoto, Y. Watanabe, Y. Miyake and A. Ono, *Angew. Chem., Int. Ed.*, 2009, **48**, 1648–1651.
36 M. S. Wysor and R. E. Zollinhofer, *Chemotherapy*, 1972, **17**, 188–199.
37 M. I. Gelfman and N. A. Kustova, *Zh. Neorg. Khim.*, 1970, **15**, 92–96.
38 A. Takashi, M. T. Ken, I. Hikaru and S. Yukiyoshi, *Bull. Chem. Soc. Jpn.*, 1989, **62**, 1078–1080.
39 Z. Assefa, B. G. McBurnett, R. J. Staples and J. P. Fackler, *Inorg. Chem.*, 1995, **34**, 4965–4972.
40 R. Uson, A. Laguna, M. Laguna, D. A. Briggs, H. H. Murray and J. P. Fackler, *Inorg. Synth.*, 1989, **26**, 85–91.
41 E. Vergara, S. Miranda, F. Mohr, E. Cerrada, E. R. T. Tiekink, P. Romero, A. Mendia and M. Laguna, *Eur. J. Inorg. Chem.*, 2007, 2926–2933, DOI: **10.1002/ejic.200700112**.
42 D. J. Daigle, A. B. Pepperma and S. L. Vail, *J. Heterocycl. Chem.*, 1974, **11**, 407–408.
43 D. J. Darensbourg, C. G. Ortiz and J. W. Kamplain, *Organometallics*, 2004, **23**, 1747–1754.
44 F. Joo, J. Kovacs, A. Katho, A. C. Benyei, T. Decuir, D. J. Darensbourg, A. Miedaner and D. L. Dubois, in *Inorg. Synth*, ed. M. Y. Darensbourg, 1998, vol. 32, pp. 1–8.
45 N. Markova, V. Enchev and G. Ivanova, *J. Phys. Chem. A*, 2010, **114**, 13154–13162.
46 G. S. Abdrakhimova, M. Y. Ovchinnikov, A. N. Lobov, L. V. Spirikhin, S. P. Ivanov and S. L. Khursan, *J. Phys. Org. Chem.*, 2014, **27**, 876–883.
47 T. L. Brown and K. J. Lee, *Coord. Chem. Rev.*, 1993, **128**, 89–116.
48 L. R. Moore, E. C. Western, R. Craciun, J. M. Spruell, D. A. Dixon, K. P. O'Halloran and K. H. Shaughnessy, *Organometallics*, 2008, **27**, 576–593.
49 D. J. Darensbourg, J. B. Robertson, D. L. Larkins and J. H. Reibenspies, *Inorg. Chem.*, 1999, **38**, 2473–2481.
50 I. Pavel, S. Cota, S. Cinta-Pinzaru and W. Kiefer, *J. Phys. Chem. A*, 2005, **109**, 9945–9952.
51 K. Dobrosz-Teperek, Z. Zwierzchowska, W. Lewandowski, K. Bajdor, J. C. Dobrowolski and A. P. Mazurek, *J. Mol. Struct.*, 1998, **471**, 115–125.
52 V. K. Rastogi and M. A. Palafox, *Spectrochim. Acta, Part A*, 2011, **79**, 970–977.
53 J. F. Villa, J. Gelber, N. Khoe and J. Cepeda, *J. Am. Chem. Soc.*, 1978, **100**, 4305–4307.
54 S. M. Meier-Menches, B. Aikman, D. Döllerer, W. T. Klooster, S. J. Coles, N. Santi, L. Luk, A. Casini and R. Bonsignore, *J. Inorg. Biochem.*, 2020, **202**, 110844.
55 V. Singh, M. Brecik, R. Mukherjee, J. C. Evans, Z. Svetlíková, J. Blaško, S. Surade, J. Blackburn, D. F. Warner, K. Mikušová and V. Mizrahi, *Chem. Biol.*, 2015, **22**, 63–75.
56 F. Sedlmayer, A. K. Woischnig, V. Unterreiner, F. Fuchs, D. Baeschlin, N. Khanna and M. Fussenegger, *Nucleic Acids Res.*, 2021, **49**, e73.
57 A. Frei, J. Zuegg, A. G. Elliott, M. Baker, S. Braese, C. Brown, F. Chen, C. G. Dowson, G. Dujardin, N. Jung, A. P. King, A. M. Mansour, M. Massi, J. Moat, H. A. Mohamed, A. K. Renfrew, P. J. Rutledge, P. J. Sadler, M. H. Todd, C. E. Willans, J. J. Wilson, M. A. Cooper and M. A. T. Blaskovich, *Chem. Sci.*, 2020, **11**, 2627–2639.
58 M. Michaut, A. Steffen, J. M. Contreras, C. Morice, A. Paulen, I. J. Schalk, P. Plésiat and G. L. A. Mislin, *Bioorg. Med. Chem. Lett.*, 2020, **30**, 127098.
59 A. M. de Almeida, B. A. de Oliveira, P. P. de Castro, C. C. de Mendonça, R. A. Furtado, H. D. Nicolella, V. L. da Silva, C. G. Diniz, D. C. Tavares, H. Silva and M. V. de Almeida, *BioMetals*, 2017, **30**, 841–857.
60 J. Stenger-Smith, I. Chakraborty and P. K. Mascharak, *J. Inorg. Biochem.*, 2018, **185**, 80–85.
61 M. K. Tizotti, R. Hörner, A. G. O. de Freitas, C. B. Kempfer, A. Bottega, J. N. Rodrigues, V. M. Cóser, A. Locatelli, G. Paraginski, C. Giacomelli and M. Hörner, *Inorg. Chim. Acta*, 2016, **441**, 78–85.
62 S. Thangamani, H. Mohammad, M. F. N. Abushahba, T. J. P. Sobreira, V. E. Hedrick, L. N. Paul and M. N. Seleem, *Sci. Rep.*, 2016, **6**, 22571.
63 C. Attila, A. Ueda and T. K. Wood, *Appl. Microbiol. Biotechnol.*, 2009, **82**, 525–533.

This journal is © The Royal Society of Chemistry 2023